Feedback between melt percolation and deformation in an exhumed lithosphere-asthenosphere boundary

Véronique Le Roux, Andrea Tommasi, Alain Vauchez

Please cite this article as: Le Roux, V., et al., Feedback between melt percolation and deformation in an exhumed lithosphere–asthenosphere boundary, Earth Planet. Sci Lett. (2008), 274: 401-413 doi:10.1016/j.epsl.2008.07.053

Feedback between melt percolation and deformation in an exhumed lithosphere–asthenosphere boundary

V. Le Roux [a,b,*], A. Tommasi [a], A. Vauchez [a]

[a] Université Montpellier II, Géosciences Montpellier, CNRS, UMR 5243, Place Eugène Bataillon, CC060 34095 Montpellier, France
[b] Macquarie University, GEMOC ARC National Key Centre, NSW 2113, Sydney, Australia

ARTICLE INFO

Article history:
Received 19 February 2008
Received in revised form 18 July 2008
Accepted 25 July 2008
Available online xxxx

Editor: C.P. Jaupart

Keywords:
melt percolation
strain localization
mantle lithosphere
olivine
pyroxene
crystal-preferred orientation
dislocation creep
diffusion
refertilization reactions, lherzolites
websterites
harzburgites
melt segregation

ABSTRACT

Interactions between deformation and melt percolation yield important consequences for the evolution of the mantle lithosphere, controlling its composition and mechanical behavior. In the Lherz massif (Pyrenees, France), the analysis of structural relationships between harzburgites, lherzolites and pyroxenites and of the crystal-preferred orientations (CPO) of olivine and pyroxenes highlights a strong feedback between percolation of basaltic melts and deformation under near-solidus conditions at the lithosphere–asthenosphere boundary. Elongated harzburgite bodies up to tens of meters wide, which are the remnants of an old lithospheric mantle, preserve a constant foliation. This foliation is locally outlined by cm-scale flattened websteritic lenses. At the contact with the enclosing lherzolites, the harzburgite foliation is crosscut by the lherzolites foliation and by cm-wide websterite bands parallel to the contact. Strain intensity in the lherzolites increases with distance to the harzburgites. Based on these observations, we propose that reactive percolation was synchronous to the deformation and propose that variations in instantaneous melt fraction, due to pyroxenes and spinel crystallization during reactive melt transport, guided strain localization. Accordingly, the observed decrease in olivine CPO intensity and change in CPO patterns from harzburgites to distal lherzolites are interpreted as recording changes in the relative contribution of dislocation glide and diffusion processes, which is ruled by a balance between the instantaneous melt fraction and the local strain rate. We also propose that the pervasive websteritic layering in the refertilized lherzolites may result from deformation-assisted melt segregation in a system with decreasing permeability due to refertilization reactions. Finally, we discuss the possible timing and geodynamical context of the refertilization episode.

1. Introduction

The evolution of the upper mantle is strongly associated with partial melting and refertilization processes. Recent studies have shown that percolating melts may react with the mantle lithosphere, inducing enrichment in fusible components, i.e., refertilization via the crystallization of pyroxenes and spinel (Rampone et al., 1994; Lenoir et al., 2001; Müntener et al., 2004; Tommasi et al., 2004; Beyer et al., 2006; Le Roux et al., 2007). Experimental deformation of partially molten assemblages shows that the presence of melt, even in low fractions, leads to a strong decrease in viscosity (Hirth and Kohlstedt, 1995; Rosenberg and Handy, 2005; Takei, 2005). Additionally, deformation may produce a higher transient permeability and facilitate melt segregation (Rosenberg and Handy, 2000; Holtzman et al., 2003). This feedback between melt percolation and deformation, observed experimentally, has also been proposed, on the basis of structural observations, as responsible for the development of shear zones in the middle and the lower crust (Tommasi et al., 1994; Brown and Solar, 1998; Kisters et al., 1998; Vauchez and Tommasi, 2003) and in the shallow mantle (Kelemen and Dick, 1995). At the plate scale, it has also been suggested, based on geodynamical models and seismic anisotropy data, that magmas play an essential role in the initiation of rifting (Buck, 2006; Kendall et al., 2006) and in the erosion of the lithosphere above mantle plumes (Thoraval et al., 2006). Interactions between melt percolation and deformation in the mantle are thus major processes in the evolution of the lithosphere, controlling its composition and mechanical behavior. In this article we document still poorly understood feedback processes between melt percolation and deformation in a complex natural system: a propagating lithosphere–asthenosphere boundary.

The Lherz Massif (Pyrenees, France) is an ideal location to study interactions between percolation and deformation in mantle rocks. It is composed of refertilized spinel lherzolites containing frequent cm-scale websteritic layers that surround metric to decametric-scale

bodies of depleted harzburgite in the southern part of the massif. Detailed structural mapping and geochemical analysis show that the lherzolites formed at the expense of the harzburgites during a near-solidus refertilization reaction coeval with deformation of the lherzolites (Le Roux et al., 2007). The Lherz massif represents therefore an outcrop of a frozen lithosphere–asthenosphere boundary where the percolation of basaltic melts deeply modified the structure and the composition of the mantle lithosphere.

We present a detailed study of the lithological distribution and deformation structures from the massif to the thin section scale, combined with analyses of olivine and pyroxenes crystal-preferred orientations (CPO) in harzburgites, refertilized lherzolites and websterites from the Lherz massif. These observations associated with previous data on the refertilization process (Le Roux et al., 2007) highlight a strong feedback between reactive melt percolation and deformation during refertilization. This results in both strain localization, which allowed the preservation of the pre-existing structure in the harzburgite lenses, and melt segregation, which lead to the formation of the websterites. Finally, we discuss the possible timing and geodynamical context for the refertilization episode.

2. The Lherz peridotitic massif (Pyrenees, France)

The Lherz Massif, type-locality of the lherzolite, is one of the largest of the 40 ultramafic bodies that outcrop along the North Pyrenean Fault (NPF; Pyrenees, France; Fig. 1a). The Pyrenean peridotite massifs, which dimensions vary from several m^2 to a few km^2, with ~1 km2 for the Lherz massif (Monchoux, 1971; Fabriès et al., 1991), are mainly composed of layered spinel lherzolites. Exhumation of Pyrenean peridotites is usually ascribed to lithospheric thinning associated with successive opening and closing of elongated, asymmetrical pull-apart basins in response to the dominantly transcurrent motion of the Iberian plate relative to the European plate in the mid-Cretaceous (Choukroune and Mattauer, 1978; Vielzeuf and Kornprobst, 1984; Debroas, 1987). Most ultramafic massifs outcrop within carbonate rocks of Jurassic to Aptian age affected by a low pressure-high temperature metamorphism that characterizes the 'North Pyrenean Metamorphic Zone' (Golberg and Leyreloup, 1990), and they are generally associated with crustal granulites (Azambre and Ravier, 1978; Pin and Vielzeuf, 1983; Vielzeuf and Kornprobst, 1984). Emplacement of the ultramafic rocks in the crust has been dated at 105–110 Ma (Henry et al., 1998). In the Lherz massif, the last stage of exhumation of the peridotites is marked by extensive brecciation in the outer rim of the peridotite body and in the host limestones that show structures typical of sedimentary reworking (Lagabrielle and Bodinier, 2008).

Although mainly composed of refertilized spinel lherzolites that form ca. 75% of the massif (Fig. 1b), the Lherz massif displays metric to decametric-scale intermingling of secondary lherzolites and highly refractory harzburgites in its topographically higher, southern part (Le Roux et al., 2007). The northern part of the massif is essentially composed of refertilized lherzolites containing a pervasive cm-scale websteritic layering (Fig. 2c,d). The websteritic bands are numerous in lherzolites, whereas harzburgites are devoid of them, except at the

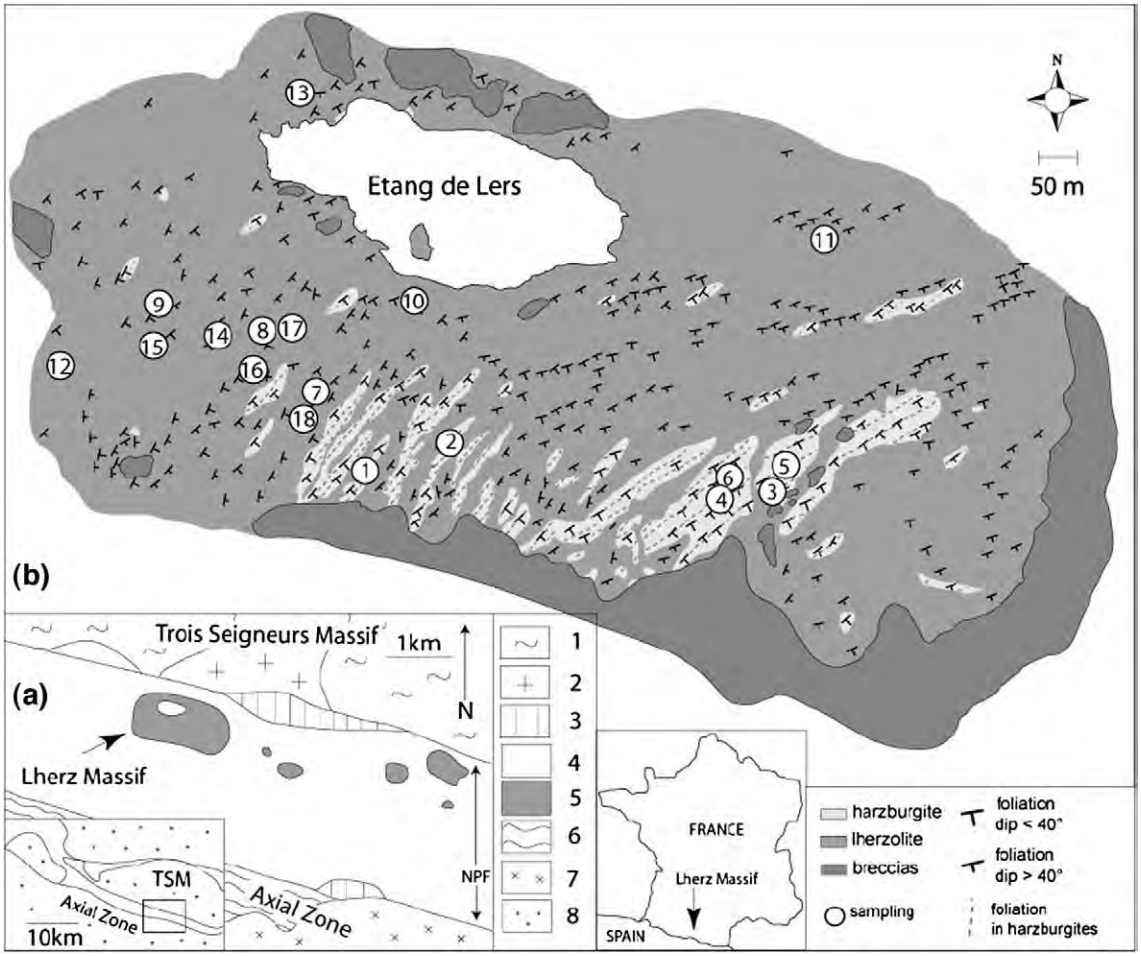

Fig. 1. (a) Localization and geological context of the Lherz Massif (Azambre and Ravier, 1978; Kornprobst and Vielzeuf, 1984; Monchoux, 1970; Vielzeuf, 1980). 1 — Schists; 2 — Mesozoic and Cenozoic rocks; 3 — Granulites; 4 — Metamorphic Mesozoic rocks; 5 — Peridotites; 6 — Granulite occurrences; 7 — Hercynian basement; 8 — Late Tertiary sediments. (b) Geological map of the Lherz Massif (Le Roux et al., 2007) with the location of analyzed samples.

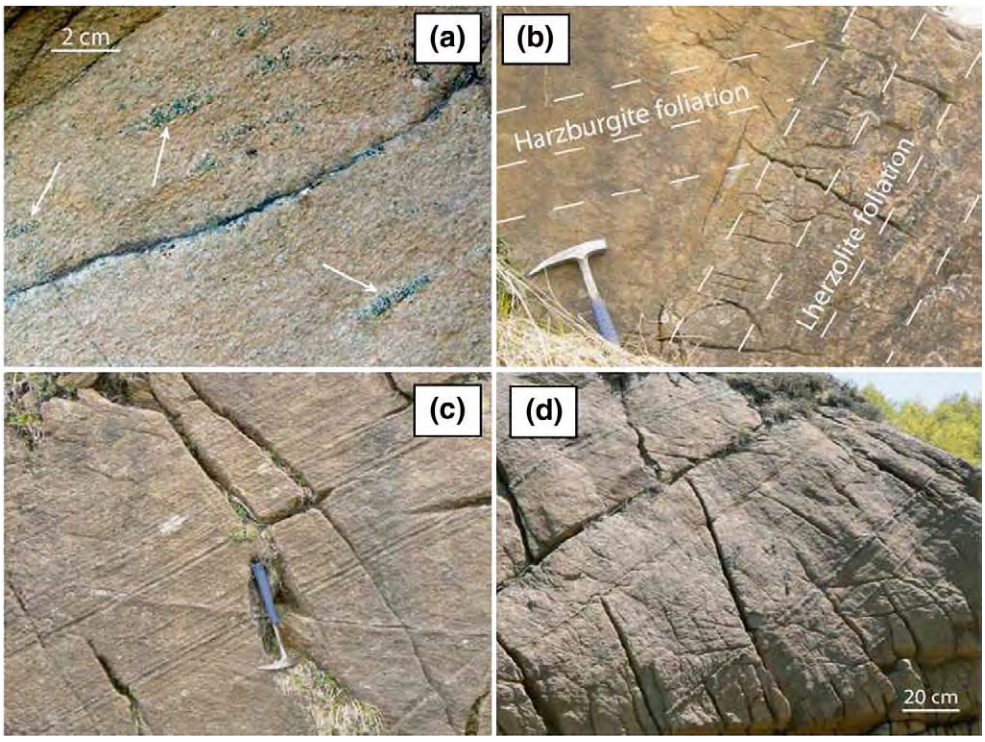

Fig. 2. Photographs of (a) fertile pockets in harzburgites; (b) a contact between harzburgite and lherzolite underlined by a thin websteritic layering. The foliations of harzburgites and lherzolites and the direction of the websteritic layering measured on the field are reported on the photograph as dashed lines; (c), (d) pervasive websteritic layering in distal lherzolites.

contact between the two lithologies. The entire massif is crosscut by a later generation of amphibole-bearing pyroxenite dykes and hornblendite veins, related to alkaline magmatism during the Cretaceous (Loubet and Allègre, 1982; Golberg et al., 1986; Bodinier et al., 1987a; Vétil et al., 1988). Meter-scale low-temperature mylonitic bands crosscut the massif; they are more common at its borders and are probably related to the emplacement of the massif in the crust (Costa and Maluski, 1988).

The harzburgites generally occur as elongated bands a few meters to tens of meters-wide within the lherzolites. All harzburgites show a penetrative shallowly-dipping foliation with a constant N40–N60°E orientation and SW–NE sub-horizontal lineation, marked by elongated spinels and elongated olivine porphyroclasts. Throughout the massif, harzburgites display a homogeneous coarse-grained porphyroclastic microstructure (Fig. 3a), characteristic of deformation by dislocation creep under high-temperature, low-stress conditions (T>1100 °C). Large olivine porphyroclasts (up to 5 mm long) are usually elongated; aspect ratios may attain up to 1:4. They display curvilinear grain boundaries, wavy extinction, and closely-spaced (100) subgrain boundaries. Orthopyroxenes and rare clinopyroxenes are smaller (2–3 mm and <1 mm on average, respectively) and show irregular shapes and wavy extinction.

Harzburgites often contain cm-scale disk-like pockets enriched in orthopyroxene–clinopyroxene–spinel flattened parallel to the foliation (Figs. 2a, 4a). In these fertile pockets, orthopyroxene is strongly deformed with common kink bands that locally evolve into fractures filled with clinopyroxene (Fig. 4c). Clinopyroxene deformation varies from grain to grain, some crystals show wavy extinction whereas others do not display any intracrystalline deformation features. Spinels display irregular interstitial shapes, which evolve into thin films along grain boundaries (Fig. 4b). Preservation of these delicate interstitial crystallization morphologies, marked by the crystallographic continuity between crystals within triple junctions and thin films along grain boundaries indicate that these crystals have not been deformed. In addition, some irregularly-shaped spinels, which surround the pyroxenes, may have formed by exsolution from the pyroxenes at even lower temperatures during cooling. According to their compositions, minerals constituting these pockets are in equilibrium with the harzburgitic matrix and represent accumulated newly-formed crystals. Approaching the contact with the lherzolites, these websteritic pockets become larger and more numerous and evolve to irregular or vein-like shapes oblique to the harzburgite foliation, but sub-parallel to the contact.

The contact between harzburgites and lherzolites is often sharp, steeply-dipping and marked by cm-scale websteritic layers (Fig. 2b) that crosscut the harzburgite foliation (Figs. 1, 2b). However, a progressive transition within some meters from harzburgite to clinopyroxene–poor lherzolites and to lherzolite may be locally observed. In the lherzolites close to the contact, the foliation is marked by a weak alignment of interstitial, irregularly-shaped spinels. This foliation is incipient close to the contact (<1 m), but it strengthens away from it, where it is marked by alignment of spinels and elongation of olivine and pyroxene crystals (Fig. 3b). It is variable in orientation (N10 to N80) and dips either eastward or southward. It is usually oblique to the harzburgite foliation and parallel to the lherzolite–harzburgite contacts. At the contact, lherzolites often display a mm- to cm-scale websteritic layering parallel to the foliation. Proximal lherzolites show coarse pyroxene grains: orthopyroxenes are 2–3 mm large on average, but may attain up to 5 mm, and clinopyroxenes are 1–2 mm large on average. Most pyroxenes are undeformed, but some display a faint wavy extinction. Olivine porphyroclasts (3–4 mm on average) are associated with smaller olivine grains (<1 mm). All olivine grains display wavy extinction and subgrains and they are more elongated with increasing distance to the contact.

Farther from the contact with the harzburgite bodies (>30 m), distal refertilized lherzolites are associated with a pervasive mm- to tens of cm-scale websteritic layering that parallels the foliation plane. Distal lherzolites are characterized by a well-developed, steeply-dipping foliation, dominantly oriented N40–N80, and defined by the

Please cite this article as: Le Roux, V., et al., Feedback between melt percolation and deformation in an exhumed lithosphere–asthenosphere boundary, Earth Planet. Sci Lett. (2008), doi:10.1016/j.epsl.2008.07.053

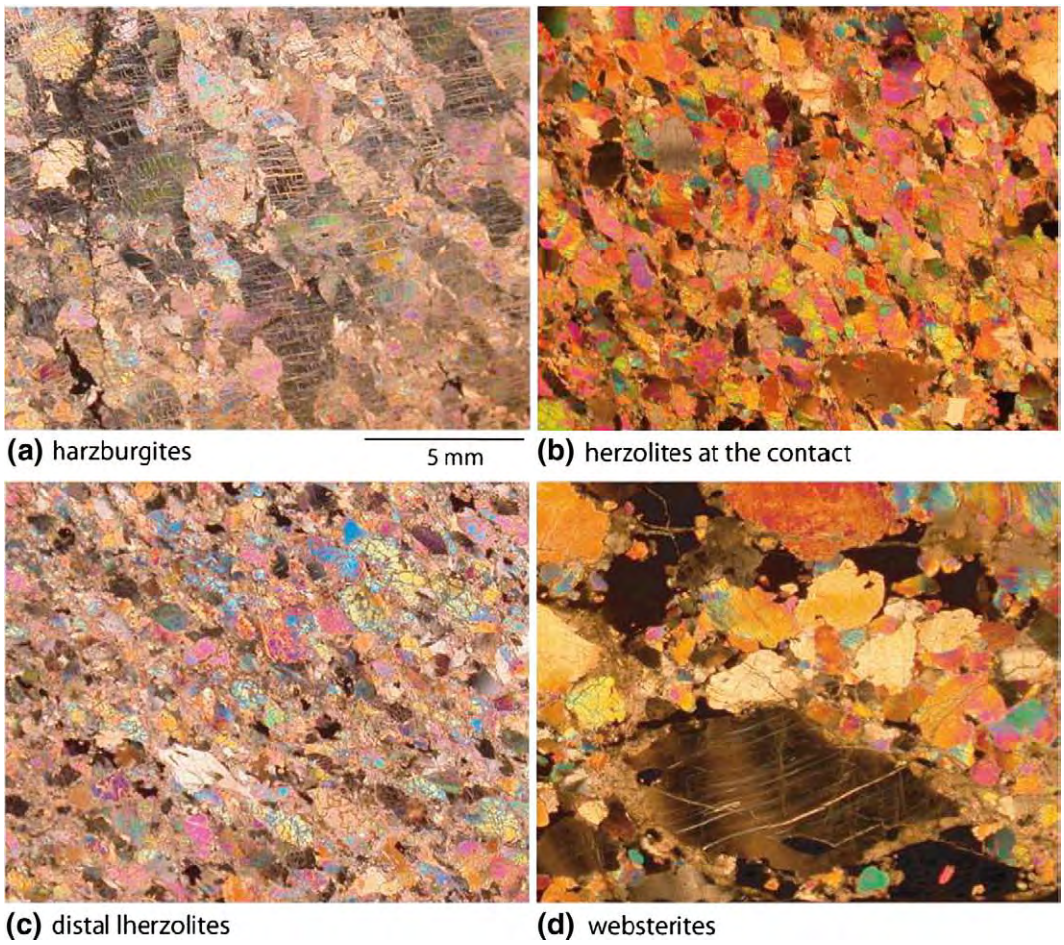

Fig. 3. Polarized-light photomicrographs showing: (a) the porphyroclastic texture in harzburgites; (b) the granular texture in lherzolites at the contact with an incipient foliation; (c) the porphyroclastic texture in distal lherzolites with well-developed foliation and lineation, marked by the elongation of spinel (Spl) and olivine (Ol) crystals; and (d) the coarse–granular texture in websterites with large deformed orthopyroxenes (Opx).

alignment of spinel aggregates and the shape preferred orientation of olivine porphyroclasts (Fig. 3c). These lherzolites display both elongated olivine porphyroclasts (3–4 mm on average) with marked wavy extinction and closely-spaced subgrain boundaries, and smaller deformed olivine grains (<1 mm). Clinopyroxenes and orthopyroxenes are equant, 2–4 mm wide, and show wavy extinction. The thickest websterite bands (>10 cm wide) are locally folded or boudinaged, suggesting that they behaved as stiffer layers during the late stages of deformation. Generally, websterite layers contain small and equant olivine grains (<1 mm) showing wavy extinction. Clinopyroxenes and orthopyroxenes are 3–4 mm on average, but orthopyroxene may attain up to 1 cm (Fig. 3d). The largest orthopyroxene and clinopyroxene crystals usually show strong wavy extinction and subgrains. Spinels display irregular shapes.

3. Evolution of CPO through the Lherz massif

3.1. Sampling and methods

To investigate the evolution of the deformation in refertilized lherzolites and associated websterites through the Lherz massif, we sampled harzburgite–lherzolite contacts, proximal lherzolites close to the contacts with harzburgites (<30 m), distal lherzolites (>30 m from the contact) and their associated websterites in the western part of the massif where they dominate (Fig. 1b).

Crystal-preferred orientations (CPO) of olivine, orthopyroxene and clinopyroxene were measured by indexing of Electron Back Scattered Diffraction (EBSD) patterns using the SEM-EBSD system at Geosciences Montpellier (France). Indexing was performed either manually or automatically. Manual measurements consisted of grain-by-grain indexing along 2 mm-spacing profiles parallel to the long axis of the thin section. For each thin section, except in the websterites, ≥200 olivine grains were indexed to obtain a statistically representative sampling of the CPO (Ben Ismaïl and Mainprice, 1998). The automatic mapping used a regular grid step of 85 μm, which is in average 10–11 times smaller than the largest observed grains, over the whole thin section. Raw maps are characterized by 50–60% indexed surface. Non-indexed pixels are linked to serpentinization, polishing defects, grain boundaries and non-indexed minor phases like spinels. Post-acquisition data treatment allowed to further increase the indexing rate by (i) filling the non-indexed pixels that have up to 8 identical neighbors with this orientation, (ii) repeating this operation using respectively 7, 6, and 5 identical neighbors, (iii) identifying the grains, i.e. continuous domains characterized by an internal misorientation <15°, and (iv) within each olivine crystal, searching and correcting for systematic indexing errors due to the olivine hexagonal pseudo-symmetry, which results in similar diffraction patterns for orientations differing by a rotation of 60° around [100]. At each step, the resulting orientation maps were checked to avoid over-extrapolation of the data. In addition, the microstructure and average grain size estimated from the EBSD crystal orientation maps were constrained by comparison to those observed by optical microscopy.

Pole figures are represented using average Euler angles for each grain instead of individual measurements to avoid over-representation of larger grains on the thin section. In addition we set up a minimum grain area of 36,125 μm^2 (5 contiguous measurement

Please cite this article as: Le Roux, V., et al., Feedback between melt percolation and deformation in an exhumed lithosphere–asthenosphere boundary, Earth Planet. Sci Lett. (2008), doi:10.1016/j.epsl.2008.07.053

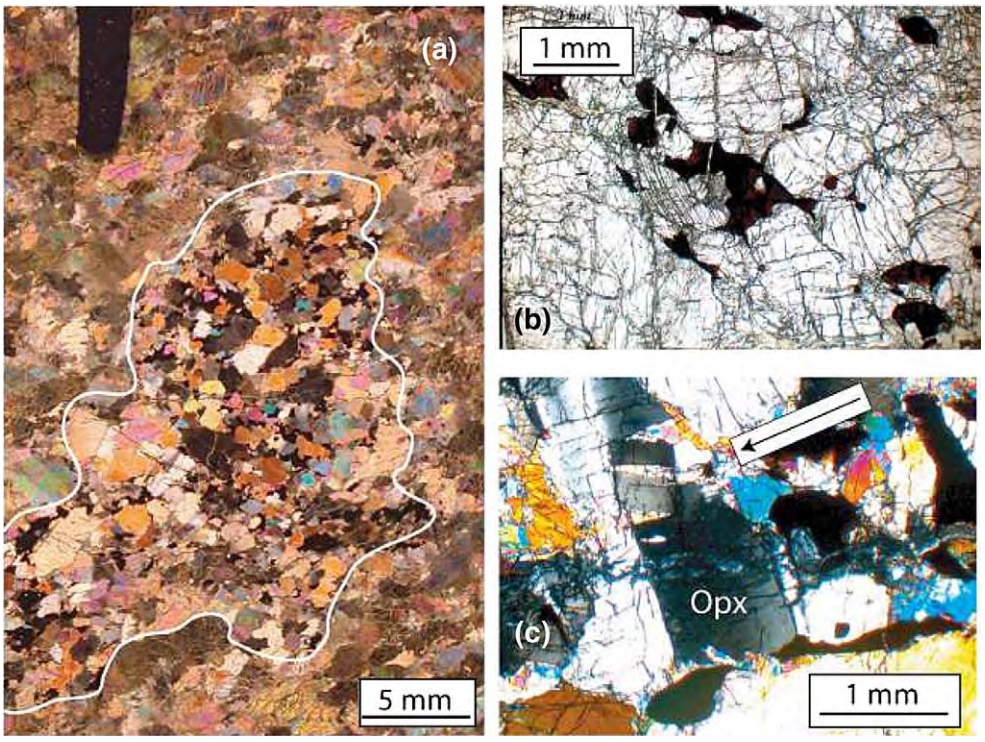

Fig. 4. (a) Photomicrograph parallel to the foliation plane of a porphyroclastic harzburgite showing a orthopyroxene–clinopyroxene–spinel rich websteritic lens with a coarse granular texture. Detail photomicrographs of the lens showing (b) irregularly-shaped interstitial spinels (Spl) and (c) a strongly deformed orthopyroxene (Opx) with en-echelon fractures normal to the kink bands filled with clinopyroxene.

points) to avoid over-representing poorly indexed grains. This minimum area is small enough not to lose information on the orientation of the smaller grains, which are on average 1 mm-wide. We obtained >400 indexed olivine grains and >200 indexed pyroxenes for each thin section, with exception of the websterites where fewer olivine grains could be measured.

The fabric strength is quantified by the *J* index, which is the volume-averaged integral of the squared orientation densities and hence is sensitive to peaks in the orientation distribution function (Bunge, 1982). *J* is dimensionless; it is 1 for a random distribution and infinity for a single crystal orientation. It usually ranges between 2 to 20 for natural peridotites (Ben Ismaïl and Mainprice, 1998).

3.2. Weakening of CPO associated with the refertilization process

Harzburgites display a clear [100]-fiber olivine CPO throughout the massif (Figs. 5a, 6 and 7). This olivine CPO pattern is characterized by alignment of [100] axes close to the lineation and a girdle distribution of [010] and [001] with a maximum of [010] normal to the foliation. It is typical of deformation by dislocation creep with activation of the high temperature, low stress (0kl)[100] slip systems, with (010) as the dominant slip plane (Tommasi et al., 2000). The orientation of the olivine CPO in the harzburgites is consistent throughout the massif. Its intensity, characterized by J_{ol} (Table 1) varies from point to point; CPO are strong (J_{ol}>8) away from the contacts, but more variable (J_{ol} varying from 10 to 4, with an average close to 7) within 10 m of the contacts (Fig. 7). Orthopyroxene CPO in the harzburgites display strong [001]-fiber patterns (Fig. 8a), characterized by alignment of [001] axes close to the lineation and a weaker concentration of [100] axes normal to the foliation (Fig. 8a). This CPO is typical of high-temperature deformation of orthopyroxene with dominant activation of the (100)[001] slip system. The correlation between olivine and orthopyroxene CPO, marked by parallelism of the dominant high-temperature Burgers vectors [100] and [001] respectively, suggests a coherent deformation of these two mineral phases. Although more dispersed, clinopyroxenes CPO are similar to that of the orthopyroxenes (Fig. 8a).

The harzburgite–lherzolite contacts are marked by a significant decrease of the olivine CPO from the harzburgites to the lherzolites with J_{ol} varying from 7 on average in harzburgites to 4 in lherzolites within a few meters (Table 1; Fig. 7). Most lherzolites at the contact have a weak [010]-fiber olivine CPO pattern (Figs. 6 and 7). Surprisingly, in lherzolites within 1 m from the contact, olivine (010) planes and pyroxenes (100) planes are not parallel to the incipient foliation measured in the field; they are rather aligned with the foliation and the olivine CPO in the neighboring harzburgites. Farther away from the contact (>1 m), the olivine CPO becomes consistent with the lineation and foliation observed in the lherzolites at both field and thin-section scales (Fig. 6). The re-alignment of the crystallographic axes in the newly-developed foliation seems thus belated compared to the change in modal composition in response to the refertilization process, suggesting a weak deformation at the contact. Pyroxenes CPO in proximal lherzolites is weak, but orthopyroxenes show a clear [001] maximum parallel to the lineation, whereas clinopyroxenes tend to show a weak [010] maximum and a girdle distribution of [001] normal and parallel to the foliation, respectively (Fig. 8a).

In the distal (>30 m from the contact), layered lherzolites that outcrop in the northern and western part of the Lherz massif, olivine CPO is always weak: J_{ol} ranges between 4.4 and 1.7 (J_{ol}=3 on average; Table 1 and Fig. 7). These lherzolites dominantly display [100]-fiber olivine CPO patterns (Figs. 5b and 7). [100] axes of olivine are aligned close to the lineation, whereas [010] and [001] display a girdle distribution with a maximum of [010] normal to the foliation. This crystallographic fabric is consistent with activation of (0kl)[100] slip systems with dominant slip on (010) planes. Some distal lherzolites display [010]-fiber olivine CPO, similar to those observed close to the harzburgite bodies (Figs. 5b and 7). Orthopyroxene CPO in distal lherzolites are also weak, but well-correlated with the olivine CPO (Fig. 8a). Finally, some distal lherzolites from the western part of the massif, show an olivine CPO uncorrelated to the olivine shape

Please cite this article as: Le Roux, V., et al., Feedback between melt percolation and deformation in an exhumed lithosphere–asthenosphere boundary, Earth Planet. Sci Lett. (2008), doi:10.1016/j.epsl.2008.07.053

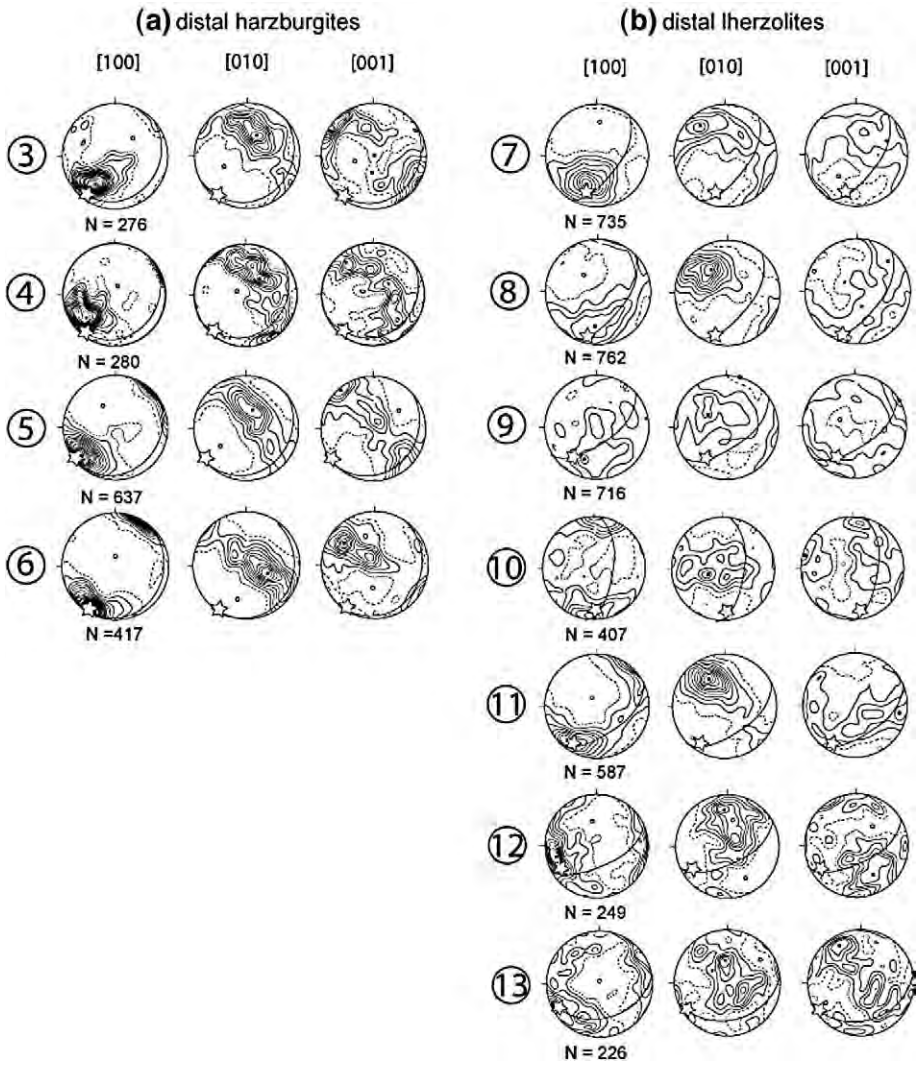

Fig. 5. (a) Olivine crystal-preferred orientations (CPO) in distal harzburgites (>15 m from the contact). (b) Olivine crystal-preferred orientations (CPO) in distal lherzolites (>30 m from the contact). Lower hemisphere equal area projections in the geographic reference frame (N at the top, E on the right). Contours at 0.5 of multiple of a uniform distribution intervals. 1 measurement per grain. *N*=Number of grains measured. Empty stars and solid lines indicate the projection of the apparent lineation and foliation, respectively.

preferred orientation that marks a clear foliation and lineation (Fig. 8b). In these peculiar lherzolites, the maximum concentration of [100] axes of olivine is oblique (ca. 40–50°) to the elongation of olivine crystals. In contrast, pyroxenes CPO show a good correlation with the olivine shape preferred orientation; [001] axes of clino- and orthopyroxenes are preferentially aligned parallel to the direction of elongation of olivine crystals (Fig. 8b).

Distal lherzolites are always associated with cm-scale websteritic layers in which olivine and pyroxene display a weak CPO (Fig. 8c). Olivine CPO is usually characterized by [010]-fiber patterns and J_{ol} varying from 3.6 to 1.7 (J_{ol}=2.6 on average; Table 1). [100] axes of olivine and [001] axes of pyroxenes are parallel to the direction of elongation of pyroxenes while [010] axes of olivine and [010] and [100] axes of clino- and orthopyroxene, respectively, are normal to the layering measured in the field.

4. Discussion

4.1. Evolution of percolation-deformation feedback mechanisms from harzburgites to lherzolites

In the Lherz massif, lherzolites formed through a refertilization process involving interaction of refractory mantle lithosphere (harzburgites) with upwelling asthenospheric melts (Le Roux et al., 2007). Detailed structural mapping shows that the orientation of the foliation and the lineation in harzburgites is consistent at the scale of the massif even though many harzburgites are small, isolated bodies enclosed in the lherzolites. On the other hand, the direction of the foliation and lineation in lherzolites varies throughout the massif. The lherzolites steeply-dipping foliation locally moulds the harzburgite bodies and often crosscuts their steady shallowly-dipping foliation. In addition, within the lherzolites, an increase in the deformation away from the contact with harzburgites is suggested by the progressive development of a shape-preferred orientation of olivine crystals and a better alignment of spinels, which results in an evolution in the field from an incipient to a well-developed foliation with increasing distance to the contacts. Stronger deformation in the distal lherzolites is also suggested by boudinage and folding of the websteritic layering that are not observed close to the contacts. These observations support that the harzburgites preserve structures related to an episode of deformation prior to the formation of the lherzolites, and that subsequent deformation was localized in the lherzolites. The important change in the deformation kinematics, characterized by sub-horizontal foliations in harzburgites to steeply-dipping foliations in lherzolites, suggests two distinct deformation episodes rather than a continuum. In the following paragraphs we discuss the relations

Please cite this article as: Le Roux, V., et al., Feedback between melt percolation and deformation in an exhumed lithosphere–asthenosphere boundary, Earth Planet. Sci Lett. (2008), doi:10.1016/j.epsl.2008.07.053

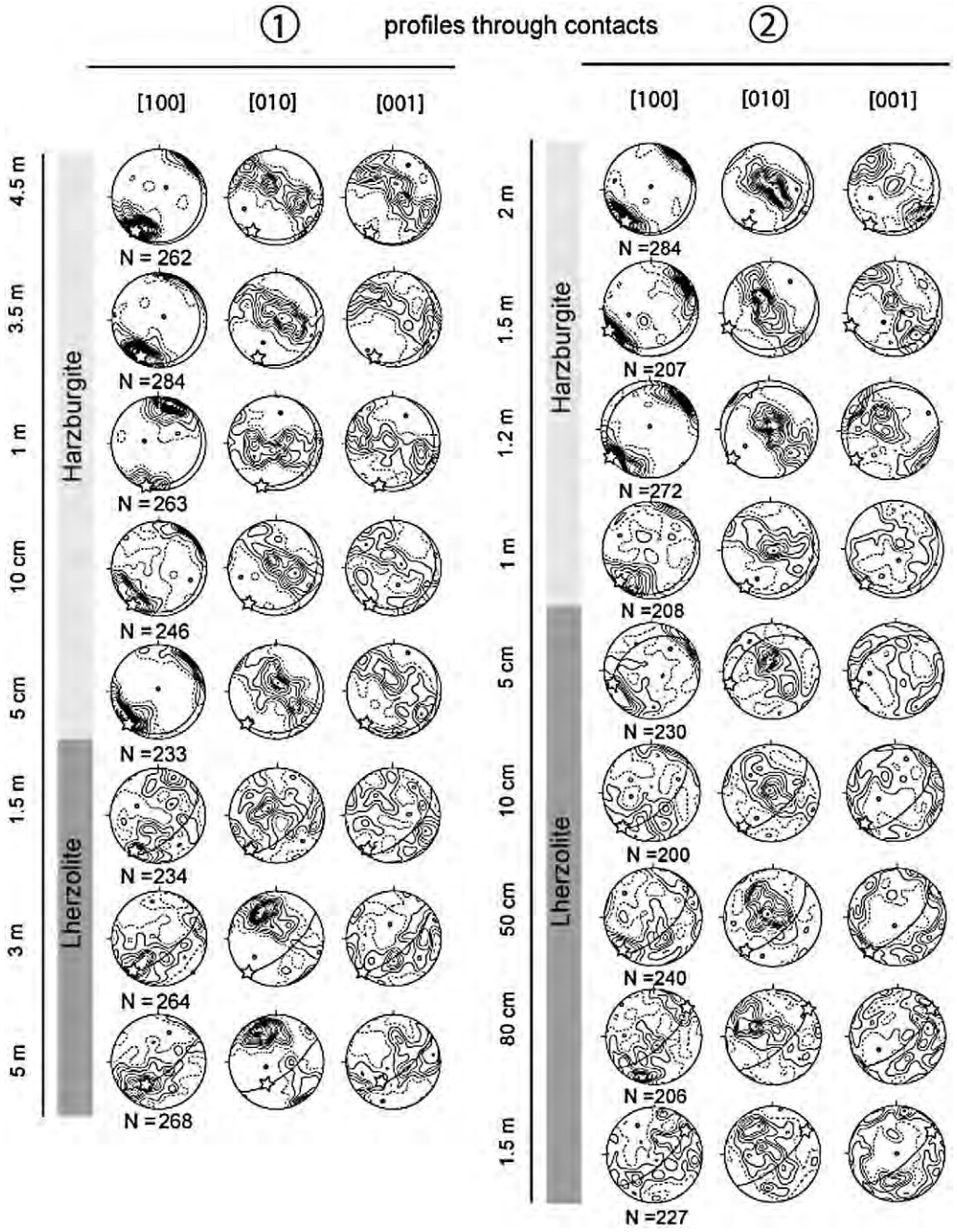

Fig. 6. Evolution of olivine crystal-preferred orientations (CPO) across two harzburgite–lherzolite contacts. Lower hemisphere equal area projections in the geographic reference frame (N at the top, E on the right). Contours at 0.5 of multiple of an uniform distribution intervals. 1 measurement per grain. *N* = Number of grains measured. Empty stars and solid lines indicate the projection of the apparent lineation and foliation, respectively.

between melt percolation and deformation that vary throughout the massif, from the harzburgites to the distal lherzolites.

The numerous cm-scale websteritic lenses in the harzburgites (Fig. 2a) were probably formed by partial crystallization of small volumes of melt injected in the harzburgite. Coexistence of strongly deformed orthopyroxene crystals showing wavy extinction, kink bands, local 'en echelon' fractures and moderately to undeformed clinopyroxenes and undeformed spinels (Fig. 4) suggests syn-kinematic crystallization where strain rate progressively decreased with increasing crystal fraction. Fractures normal to kink bands in large deformed orthopyroxene crystals filled by small undeformed clinopyroxene crystals (Fig. 4c) may have resulted from crystal-scale hydraulic fracturing in the harzburgites caused by local overpressure due to the presence of melts.

Far from the harzburgite–lherzolite contacts, these websteritic lenses are systematically parallel to the harzburgites foliation. In contrast, close to the contacts, they are larger and more numerous and they are often oblique to the harzburgite foliation and parallel to the contact. Because of their minerals composition similar to those of the host matrix, it seems difficult to chemically discriminate whether these pockets are linked or not to the refertilization event. Although a possible formation of these websteritic lenses during an older melt percolation event cannot be ruled out, we favor, based on our structural observations, the hypothesis that they represent the early stage of the melt percolation event that formed the lherzolites. In this scenario, the foliation-parallel websterite lenses represent the initial stages of melt percolation that were accompanied by an incipient deformation of the harzburgites. Alignment of the melt lenses in the

Please cite this article as: Le Roux, V., et al., Feedback between melt percolation and deformation in an exhumed lithosphere–asthenosphere boundary, Earth Planet. Sci Lett. (2008), doi:10.1016/j.epsl.2008.07.053

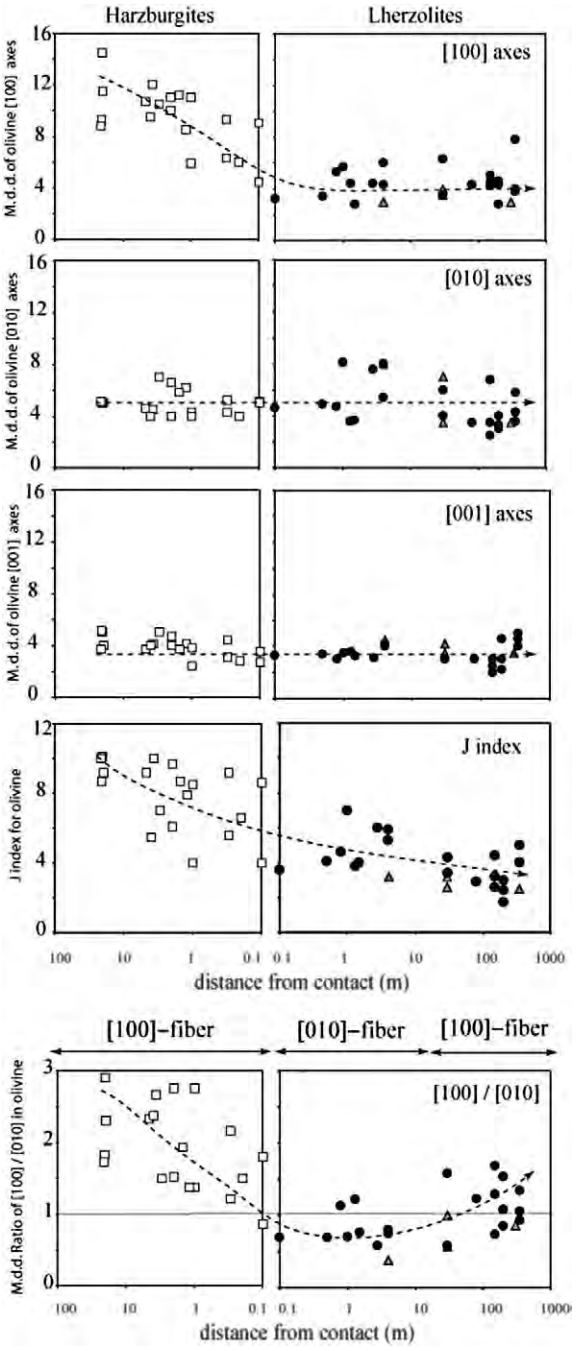

Fig. 7. Evolution of olivine CPO as function of the distance to the harzburgite–lherzolite contacts. (a) CPO strength, represented by the *J* index. (b), (c), and (d) Maximum density of distribution of [100], [010], and [001] axes of olivine, respectively. (e) Ratio of maximum density of distribution of [100] axes relative to the one of [010] axes. This plot highlights the transition from strong [100]-fiber patterns in harzburgites to ([010]-fiber patterns in lherzolites close to the contact, and finally to weak [100]-fiber patterns in lherzolites far from the contact. Empty squares: harzburgites; solid circles: lherzolites; grey triangles: websterites. Dotted lines outline the general evolution of the olivine CPO from the harzburgites to the lherzolites far from the contacts.

foliation implies that the percolation of these small melt volumes was guided by the preexistent anisotropic structure of the harzburgites (Waff and Faul, 1992; Tommasi et al., 2008). The strong olivine CPO in the harzburgites resulted in a mechanical anisotropy (Tommasi and Vauchez, 2001) that probably also controlled the incipient stages of deformation. Close to the contact with lherzolites, the structural control by the harzburgite foliation was probably overwhelmed by the external solicitation (imposed kinematics), which is better expressed in lherzolites. Finally, coexistence of deformed and undeformed minerals in these lenses suggests that partial crystallization and refertilization reactions in the melt pockets led to a stop of the deformation and transfer of strain to domains with a larger proportion of melt and hence a lower dynamic viscosity.

With increasing distance to the contacts with harzburgites, lherzolites display an evolution of macroscopic structures and crystal preferred orientations that may be explained by variations in finite strain and in the melt fraction present during deformation. The tectonic fabric of the lherzolites strengthens with increasing distance to the contact. Within 1 m from contact, the lherzolites show an incipient foliation marked by the alignment of interstitial spinels and a cm-scale websterite banding, but their olivine CPO is still parallel to the harzburgite one. This suggests that, in this narrow contact zone, strain was not high enough to erase the crystallographic fabric inherited from harzburgites. Within 30 m from the contacts, proximal lherzolites show a weak but clearly developed foliation and lineation, to which is associated a weak olivine CPO with a dominant [010]-fiber pattern, characterized by a point maximum of [010] normal to the foliation and dispersion of [100] in the foliation plane.

[010]-fiber olivine patterns similar to those observed in the proximal lherzolites have been observed in peridotites world-wide, for instance in the Ronda massif (Vauchez and Garrido, 2001), in alkali–basalt xenoliths from Siberia (Tommasi et al., 2008), in cratonic xenoliths (Ben Ismaïl and Mainprice, 2001; Vauchez et al., 2005) and in mantle xenoliths from oceanic islands (Bascou et al., 2008). The

Table 1
Modal composition and olivine CPO pattern and intensity (J index) of the studied samples, according to their distance to the nearest harzburgite–lherzolite contact

Sampling site	Sample type	Distance from contact	*J* index of olivine	Fiber	Modal composition			
					Ol	Opx	Cpx	Spl
1	Harzburgite	5 cm	8.6	[100]	79.6	17.9	1.9	0.6
1	Harzburgite	10 cm	6.6	[100]	75.3	20.8	2.2	1.7
1	Harzburgite	1 m	8.5	[100]	71.4	25.7	2.3	0.6
1	Harzburgite	3.5 m	9.2	[100]	76.9	20.3	2.1	0.7
1	Harzburgite	4.5 m	10	[100]	66.8	27.7	3.1	2.5
1	Lherzolite	1.5 m	3.8	[100]	45.5	28.5	22.7	3.3
1	Lherzolite	3 m	6	[010]	57.3	29.5	10.9	2.3
1	Lherzolite	5 m	7	[010]	54.4	28.4	15.2	2.0
2	Harzburgite	1 m	4	[100]	80.4	17.6	1.5	0.5
2	Harzburgite	1.2 m	7.9	[100]	84.1	14.1	1.4	0.4
2	Harzburgite	1.5 m	8.7	[100]	82.9	15.2	1.4	0.4
2	Harzburgite	2 m	9.7	[100]	82	16	1.5	0.6
2	Lherzolite	5 cm	4	[010]	78	16	5	1
2	Lherzolite	10 cm	3.6	[010]	68.8	19.9	9.7	1.6
2	Lherzolite	50 cm	4.6	[100]	61.6	20.8	14.9	2.7
2	Lherzolite	80 cm	4.1	[010]	72.6	16.1	9.3	1.9
2	Lherzolite	1.5 m	4	[010]	59.9	26.3	11.7	2.1
3	Harzburgite	>15 m	8.7	[100]	94.0	4.6	1.2	0.2
4	Harzburgite	>15 m	10	[100]	79.5	16.8	2.4	1.2
5	Harzburgite	>15 m	9.2	[100]	78.0	19.0	2.0	1.0
6	Harzburgite	>15 m	10.1	[100]	76.0	21.0	2.0	1.0
7	Lherzolite	30 m	4.3	[100]	61.0	25.0	11.5	2.5
8	Lherzolite	50 m	3.4	[010]	46.0	35.0	15.0	2.0
9	Lherzolite	60 m	1.75	[010]	46.0	32.0	20.0	2.0
10	Lherzolite	70 m	2.6	[100]	46.0	29.0	20.0	5.0
11	Lherzolite	150 m	4.4	[010]	63.0	19.0	15.0	3.0
12	Lherzolite	150 m	3	[100]	63.6	22.7	12.0	1.7
13	Lherzolite	350 m	4	[100]	62.0	24.0	12.0	2.0
14	Lherzolite	80 m	2.9	[100]	78.0	16.0	5.0	1.0
15	Lherzolite	80 m	3.2	[100]	60.0	25.0	12.5	2.5
16	Websterite	10 m	3.6	[010]	5.0	46.5	38.5	10.0
17	Websterite	30 m	2.3	[010]	30.0	39.0	27.0	4.0
18	Websterite	30 m	3.5	[010]	12.0	34.0	45.0	9.0

The localization of the samples is given in Fig. 1; Ol = olivine, Opx = orthopyroxene, Cpx = clinopyroxene, Spl = spinel. Modal compositions were calculated by inversion of whole-rock chemical compositions based on mineral compositions obtained by microprobe analysis (Le Roux et al., 2007).

Please cite this article as: Le Roux, V., et al., Feedback between melt percolation and deformation in an exhumed lithosphere–asthenosphere boundary, Earth Planet. Sci Lett. (2008), doi:10.1016/j.epsl.2008.07.053

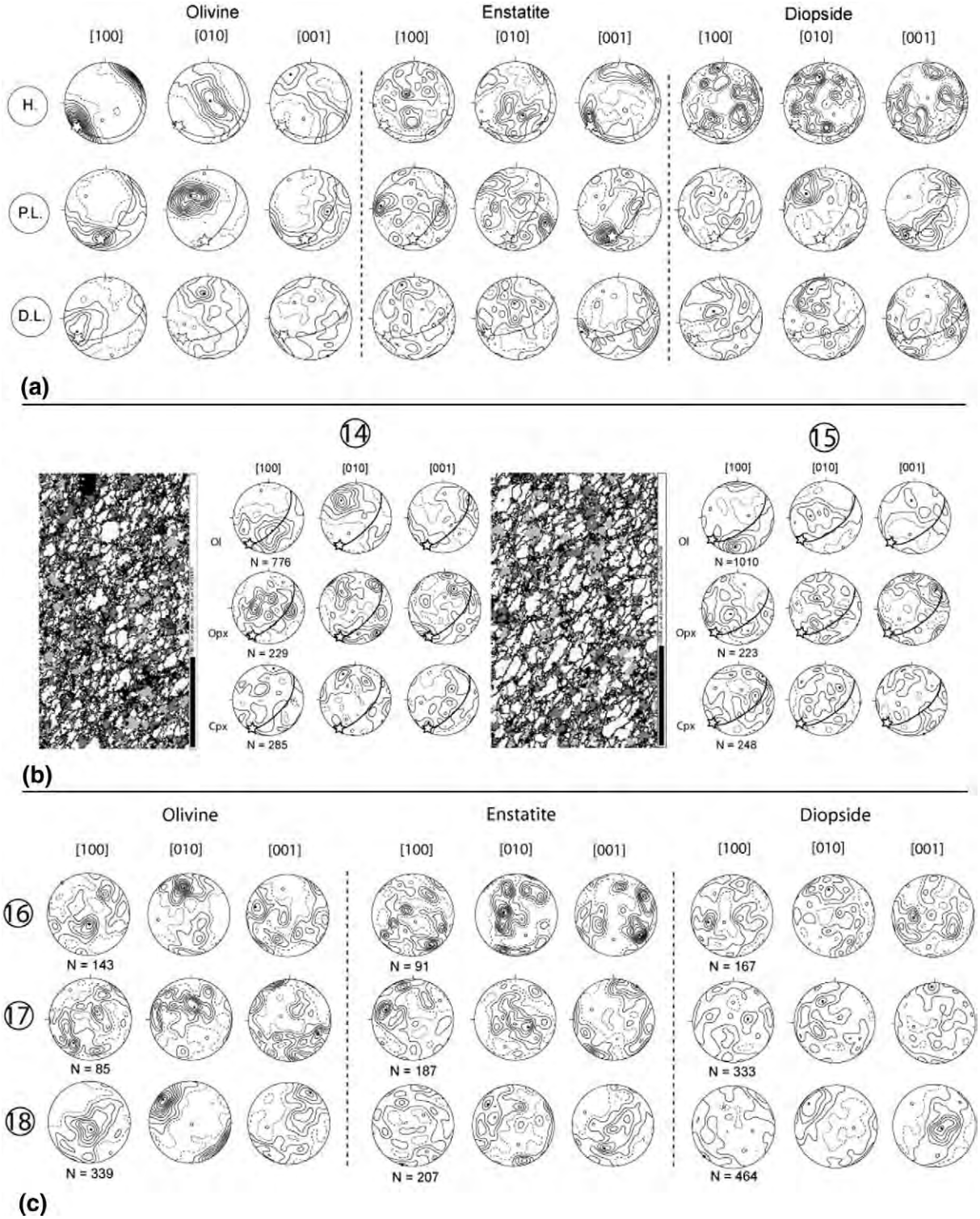

Fig. 8. (a) Representative crystal-preferred orientations (CPO) of olivine, enstatite and diopside in harzburgites (H.), proximal lherzolites (P.L.) and distal lherzolites (D.L.). Lower hemisphere equal area projections in the geographic reference frame (N at the top, E on the right). Contours at 0.5 of multiple of a uniform distribution intervals. 1 measurement per grain. *N* = Number of grains measured. Empty stars and solid lines indicate the projection of the average lineation and foliation of representative samples. (b) Shape- and crystal-preferred orientations (CPO) of olivine (Ol, white), orthopyroxene (Opx, light gray) and clinopyroxene (Cpx, dark gray) measured by crystal orientation mapping with a 85 μ m grid step in two 'abnormal' distal lherzolites. Empty stars and solid lines indicate the projection of the apparent lineation and foliation respectively. The lineation, marked by the elongation of olivine crystals, is not parallel to the maximum concentration of [100] axes of olivine, but it is parallel to the maximum concentration of [001] axes of pyroxenes. (c) Crystal-preferred orientations (CPO) of olivine, enstatite and diopside in cm-scale websterite layers within lherzolites. Dotted lines represent the orientation of the websteritic layer.

development of such patterns has been explained by: (i) axial shortening or 3D transpressive deformation (Tommasi et al., 1999; Bascou et al., 2008), (ii) activation of multiple glide directions (Tommasi et al., 2000; Mainprice et al., 2005), (iii) static recrystallization (Tommasi et al., 2008), and (iv) deformation in presence of melt (Holtzman et al., 2003). The alignment of [001] axes of orthopyroxene forming a point maximum close to the lineation does not support a transpressive deformation, which would also result in dispersion of

Please cite this article as: Le Roux, V., et al., Feedback between melt percolation and deformation in an exhumed lithosphere–asthenosphere boundary, Earth Planet. Sci Lett. (2008), doi:10.1016/j.epsl.2008.07.053

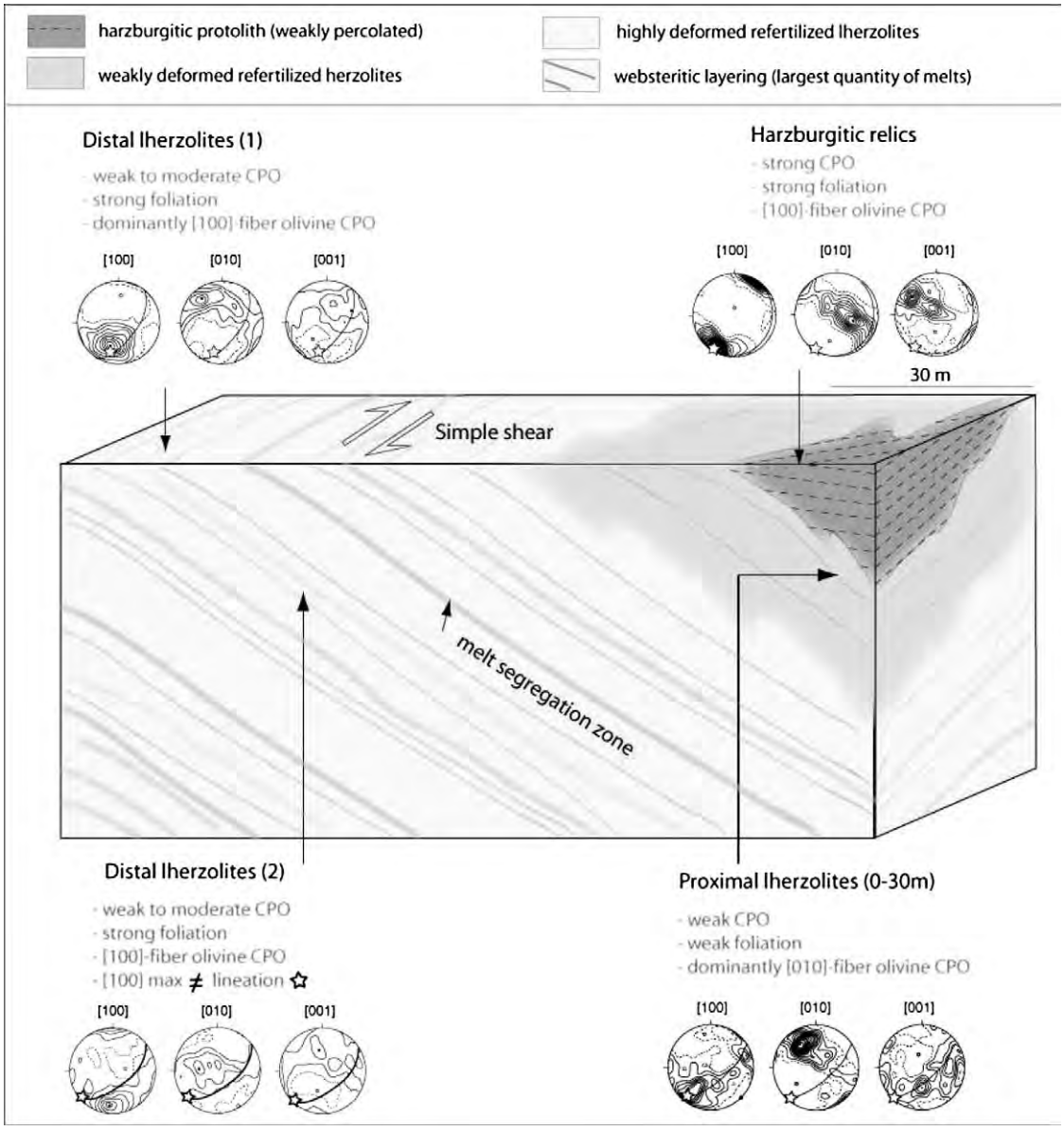

Fig. 9. Sketch summarizing the evolution of microstructures and olivine CPO in harzburgites and lherzolites from the Lherz massif according to their distance to the harzburgite–lherzolite contacts.

the orthopyroxene [001] axes in the foliation plane, as observed for instance in the Kerguelen Islands mantle (Bascou et al., 2008). The present microstructural observations indicate that the Lherz peridotites were deformed in the shallow mantle (in the spinel stability field) at near-solidus conditions. The pressure/stress conditions that prevailed during the deformation are therefore too low for activation of [001] glide (Jung and Karato, 2001; Couvy et al., 2004; Mainprice et al., 2005; Vauchez et al., 2005). Indeed, analysis of crystallographic orientation maps shows that subgrain boundaries in these lherzolites are dominantly (100) tilt boundaries, implying dominant activation of [100] glide. Finally, the absence of annealing features in olivine does not support static recrystallization. Thus we favor the latter hypothesis, i.e., a simple shear deformation in presence of melt to explain [010]-fiber olivine patterns in the proximal lherzolites. This suggests that deformation mechanisms similar to those in the laboratory experiments were activated even though natural deformation conditions were very different from the experimental ones, in particular the grain sizes (10 μm versus several mm in natural conditions) and the strain rates.

Farther from the contact (>30 m), the distal lherzolites have a well-developed foliation and lineation marked by the alignment of spinel aggregates and flattening of olivine, which suggest a larger finite strain. This interpretation is corroborated by the observation of local boudinage or folding of the pervasive websteritic layering. Paradoxically, the distal lherzolites display olivine CPO with a dominant [100]-fiber pattern (Fig. 5b), but that are significantly weaker than those in the proximal lherzolites. Higher finite strain in the distal lherzolites may have favored a better orientation of [100] parallel to the lineation. The association of a strong foliation and lineation with weak CPO might be explained by an increase of diffusion accommodated creep and/or grain boundary sliding at the expense of dislocation creep. Diffusion processes are favored by higher temperatures, lower deviatoric stresses, and the presence of fluids. An important temperature or stress gradient is unrealistic at the tens of meters scale. However the greater abundance of websteritic layers, locally up to tens of cm-wide, suggests that this zone may have experienced a higher melt flux than the proximal lherzolites, even though the porosity probably never exceeded 2–3%. Larger instantaneous melt

Please cite this article as: Le Roux, V., et al., Feedback between melt percolation and deformation in an exhumed lithosphere–asthenosphere boundary, Earth Planet. Sci Lett. (2008), doi:10.1016/j.epsl.2008.07.053

fractions may have favored melt-assisted grain boundary sliding (Rosenberg and Handy, 2001; Scott and Kohlstedt, 2006). The average olivine grain size decreases from harzburgites to refertilized lherzolites. Smaller grains have a larger surface/volume ratio which, when deformation occurs in the presence of melt, favors an accommodation by melt-assisted grain boundary sliding. Furthermore, Wark and Watson (2000) have shown that when coarse- and fine-grained domains are in chemical communication, melt is focused in the fine-grained domains, resulting in a permeability that matches or exceeds that of coarser grained domains. Thus if grain size refinement preceded melt percolation, both melt percolation and deformation may have localized within the fine-grained domains. Finally, some distal lherzolites have a maximum concentration of [100] axes at 40–50° to the lineation marked by the elongation of the olivine crystals, which is nevertheless parallel to the enstatite [001] maximum (Fig. 8b). We speculate that the observed lack of correlation between the shape- and crystallographic fabric of olivine might be related to partitioning of deformation with a higher contribution of diffusion and dislocation creep in melt-rich and melt-poor domains, respectively (Holtzman et al., 2003) or to local transtension.

Structural data in the Lherz massif points to a direct correlation between strain intensity and percolating melt volume fraction as illustrated in Fig. 9. Increasing deformation tends to favor melt segregation (Holtzman et al., 2003), which, by a feedback effect, leads to further strain localization. In the Lherz massif however, the progressive crystallization of the magmas during the refertilization reaction might have been a limitant parameter for this feedback between deformation and percolation, resulting in transfer of strain towards new melt-rich zones.

4.2. Formation of a pervasive websteritic layering in refertilized lherzolites

The refertilization process in the Lherz massif resulted in the formation of both massive lherzolites and of mm- to tens of cm-scale websteritic layers parallel to the foliation of the lherzolites. The websteritic layering is pervasive in the distal lherzolites, but cm-wide websteritic bands are also often observed at the harzburgite–lherzolite contacts. The chemical composition of these websterites shows that they do not represent simple crystallized trapped melts (Bodinier et al., 1987b). We interpret therefore these websteritic layers as zones of melt segregation, favored by strain, where higher melt fractions resulted in more developed refertilization reactions (dissolution of larger volumes of olivine and crystallization of larger amounts of pyroxenes and spinels). However, the actual volume of melts needed to form these layers cannot be assessed accurately.

Holtzman et al. (2003) showed that in olivine + basalt + chromite or FeS, anorthite + basalt, and in olivine + albite melt samples deformed under simple shear, melt segregates into a network of melt-rich bands. Analysis of these results as well as numerical models suggest that segregation is controlled by pressure gradients and depends therefore on the compaction length of the system, which is a function of the permeability and of the solid and fluid viscosities (Spiegelman, 1993; Holtzman et al., 2003; Rabinowicz and Ceuleneer, 2005). In the Lherz massif, pyroxenes and spinel crystallization during refertilization reactions resulted in a reduction of porosity, plugging the melt network and hence favoring the segregation of melts. The coexistence of cm-scale strongly deformed orthopyroxenes and moderately to undeformed clinopyroxenes suggests that the deformation slowed progressively as the newly-formed crystals plugged the porosity, likely localizing further in less crystallized domains. The websteritic layers in the Lherz massif thus probably represent multiple "frozen" timesteps of a dynamic melt transport system.

4.3. Geodynamic environment of the refertilization process

In this paper we suggest that the refertilization of the old harzburgitic mantle lithosphere was coeval with a deformation dominated by simple shear under subsolidus temperature conditions. During the evolution of the Pyrenean domain, two major events have tightly associated magmatism and deformation: 1) the Cretaceous deformation and 2) the Hercynian orogeny. The emplacement of the Lherz massif in the crust during the Cretaceous (Henry et al., 1998) might have produced such a deformation. However amphibole-pyroxenite dykes considered to represent trans-lithospheric melt conduits for Cretaceous alkaline magmatism (Loubet and Allègre, 1982; Golberg et al., 1986; Bodinier et al., 1987a; Vétil et al., 1988) crosscut at high angle the foliations of both the harzburgites and refertilized lherzolites, suggesting that the refertilization event occurred before the Cretaceous. Moreover Pyrenean peridotites record equilibrium conditions of 8–17 kb at ~950 °C suggesting an isobaric cooling stage from ~1200 °C to ~900 °C during a ~20My thermal relaxation episode (Sautter and Fabriès, 1990; Fabriès et al., 1991). This long thermal relaxation rules out the idea that the refertilization episode occurred during the emplacement of the massif in the crust, since this later is inferred to have occurred in <5 myr throughout the Pyrenees (Fabriès et al., 1991; Schärer et al., 1995; Fabriès et al., 1998).

Seismic anisotropy measurements in the Pyrenees led Barruol et al. (1998) to suggest that the retrieved S-wave polarization anisotropy is largely inherited from the deformation of the mantle lithosphere during the Hercynian orogeny. Indeed, shear-wave splitting measurements yield a consistent ~N100E polarization of the fast S-wave and rather large splitting, suggesting a lithospheric fabric mostly due to transcurrent motions. This anisotropy is observed in all domains of the Pyrenean belt, even in the southern and northern external domains where the ECORS seismic profile has shown that only the uppermost crust was involved in the Pyrenean tectonics (Choukroune, 1988). An Hercynian orogenic fabric therefore appears as the best candidate to explain the observed S-wave anisotropy (Vauchez and Barruol, 1996; Barruol et al., 1998). The late stages of the Hercynian orogeny in the Pyrenees are characterized by emplacement of syncinematic granites at the scale of the belt. Based on the analysis of the magmatic flow fabric of these granites and of the tectonic fabric in the host rocks, Gleizes et al. (1997) suggested that the whole Pyrenean belt behaved as a large, lithospheric-scale "shear-zone" during the last stage of the Variscan orogeny. We suggest therefore that the Variscan event may represent an adequate context for the syn-orogenic refertilization episode of an older lithosphere, remnants of which have been preserved in Lherz massif.

5. Conclusions

Based on a detailed study of the relationships between deformation and melt percolation in harzburgites, refertilized lherzolites and websteritic layers in the Lherz massif we propose that:

(a) Reactive percolation of basaltic melts in the harzburgitic Pyrenean lithosphere was synchronous to a lithospheric-scale simple shear deformation, which led to the development of a new foliation in the refertilized, secondary lherzolites and associated websterites. Some remnants of the harzburgitic protolith avoided most of this deformation and form elongated lenses within the refertilized and deformed lherzolites.

(b) There is a continuum in the deformation, which started in the harzburgites and progressively localized in the refertilized lherzolites. The deformation intensity increases with increasing distance from the harzburgites and increasing volume of percolating melts. We suggest that feedback between deformation and melt percolation produced the observed structures: larger melt fractions favored strain localization and larger strain favored melt percolation through a higher dynamic porosity. This feedback is probably a major process in the compositional and structural rejuvenation of the subcontinental mantle lithosphere.

Please cite this article as: Le Roux, V., et al., Feedback between melt percolation and deformation in an exhumed lithosphere–asthenosphere boundary, Earth Planet. Sci Lett. (2008), doi:10.1016/j.epsl.2008.07.053

(c) The response of the rocks' texture to deformation depends on a subtle balance between two parameters: the strain intensity and the volume of percolating melts. In the Lherz massif, this led to coexistence of [100]-fiber and [010]-fiber olivine CPO. [100]-fiber olivine CPO developed where strain dominated the evolution (very low melt fractions as in the harzburgites or high strain as in the distal lherzolites). On the other hand, [010]-fiber olivine CPO developed where melt played an equally important or dominant part in the evolution (low melt fraction and incipient strain in proximal lherzolites or large melt fractions in the websterites).

(d) The formation of the websterites layers was synchronous of that of the lherzolites, due to melt segregation that was probably favored by the refertilization reactions, which plugged the melt network, reducing the permeability and producing small-scale pressure gradients.

(e) The deformation-refertilization event observed in the Lherz massif probably records the evolution of the Pyrenean mantle lithosphere during the late stage of the Variscan orogeny during the Carboniferous, when abundant magmatism coeval with orogen-parallel transcurrent faulting was emplaced throughout the Pyrenean domain. This shearing produced a large-scale anisotropic structure in the mantle lithosphere, which may explain the belt-parallel polarization of the fast split shear wave observed in the Pyrenees.

Acknowledgments

We thank Ben Holtzman and Günter Suhr for their constructive reviews. D. Mainprice provided softwares for analysing/plotting CPO data and C. Nevado and D. Delmas supplied high quality polished thin sections for EBSD measurements. This study was partially funded by the Institut National des Sciences de l'Univers (CNRS/INSU) program 'Dynamique et Evolution de la Terre Interne' (DyETI). This is contribution no 544 from the GEMOC ARC National Key Centre.

References

Azambre, B., Ravier, J., 1978. Les écailles de gneiss du faciès granulite du Port de Saleix et de la région de Lherz (Ariège). Nouveaux témoins du socle profond des Pyrénées. Bull. Soc. Géol. Fr. XX, 221–228.

Barruol, G., Souriau, A., Vauchez, A., Diaz, J., Gallart, J., Tubia, J., Cuevas, J., 1998. Lithospheric anisotropy beneath the Pyrenees from shear wave splitting. J. Geophys. Res. 103, 30039–30053.

Bascou, J., Delpech, G., Vauchez, A., Moine, B.N., Cottin, J.-Y., Barruol, G., 2008. An integrated study of microstructural, geochemical and seismic properties of lithospheric mantle above the Kerguelen plume (Indian Ocean). Geochem. Geophys. Geosyst. 9, Q04036. doi:04010.01029/02007GC001879.

Ben Ismaïl, W., Mainprice, D., 1998. An olivine fabric database: an overview of upper mantle fabrics and seismic anisotropy. Tectonophysics 296, 145–157.

Ben Ismaïl, W., Mainprice, D., 2001. The Kaapvaal craton seismic anisotropy: petrophysical analyses of upper mantle kimberlite nodules. Geophys. Res. Lett. 28, 2497–2500.

Beyer, E., Griffin, W.L., O'Reilly, S.Y., 2006. Transformation of Archaean lithospheric mantle by refertilization: evidence from exposed peridotites in the Western Gneiss Region, Norway. J. Petrol. 47, 1611–1636.

Bodinier, J.-L., Fabriès, J., Lorand, J.-P., Dostal, J., Dupuy, C., 1987a. Geochemistry of amphibole pyroxenite veins from the Lherz and Freychinède ultramafic bodies (Ariège, French Pyrenees). Bull. Minéral. 110, 345–358.

Bodinier, J.-L., Guiraud, M., Fabriès, J., Dostal, J., Dupuy, C., 1987b. Petrogenesis of layered pyroxenites from the Lherz, Freychinède and Prades ultramafic bodies (Ariège, French Pyrenees). Geochim. Cosmochim. Acta 51, 279–290.

Brown, M., Solar, G.S., 1998. Shear-zone systems and melts: feedback relations and self-organization in orogenic belts. J. Struct. Geol. 20, 211–227.

Buck, W.R., 2006. The role of magma in the development of the Afro–Arabian rift system. Geological Society of London, Special Publications, vol. 259, pp. 43–54.

Bunge, H.J., 1982. Texture analysis in material sciences. Butterworths, London.

Choukroune, P., 1988. The ECORS deep reflection seismic survey across the Pyrenees. Nature 331, 508–510.

Choukroune, P., Mattauer, M., 1978. Tectonique des plaques et Pyrénées: sur le fonctionnement de la faille transformante nord-pyrénéenne; comparaison avec des modèles actuels. Bull. Soc. Géol. Fr. 20, 689–700.

Costa, S., Maluski, H., 1988. Use of ^{40}Ar–^{39}Ar stepwise heating method for dating mylonitic zones: an example from the St. Barthelemy Massif (Northern Pyrenees, France). Chem. Geol. 72, 127–144.

Couvy, H., Frost, D.J., Heidelbach, F., Nyilas, K., Ungar, T., Mackwell, S., Cordier, P., 2004. Shear deformation experiments of forsterite at 11 GPa–1400 °C in the multianvil apparatus. Eur. J. Mineral. 16, 877–889.

Debroas, E.J., 1987. Modèle de bassin triangulaire à l'intersection de décrochements divergents pour le fossé albo-cénomanien de la Ballongue (zone nord-pyrénéenne, France). Bull. Soc. Géol. Fr. 8, 887–898.

Fabriès, J., Lorand, J.-P., Bodinier, J.-L., 1998. Petrogenetic evolution of orogenic lherzolite massifs in the central and western Pyrenees. Tectonophysics 292, 145–167.

Fabriès, J., Lorand, J.-P., Bodinier, J.-L., Dupuy, C., 1991. Evolution of the upper mantle beneath the Pyrenees: evidence from orogenic spinel lherzolite massifs. J. Petrol. 55–76.

Gleizes, G., Leblanc, D., Bouchez, J.-L., 1997. Variscan granites of the Pyrenees revisited: their role as syntectonic markers of the orogen. Terra Nova 9, 38–41.

Golberg, J.M., Leyreloup, A.F., 1990. High temperature–low pressure Cretaceous metamorphism related to crustal thinning (Eastern North Pyrenean Zone, France. Contrib. Mineral. Petrol. 104, 194–207.

Golberg, J.M., Maluski, H., Leyreloup, A.F., 1986. Petrological and age relationship between emplacement of magmatic breccia, alkaline magmatism and static metamorphism in the North Pyrenean Zone. Tectonophysics 129, 275–290.

Henry, P., Azambre, B., Montigny, R., Rossy, M., Stevenson, R.K., 1998. Late mantle evolution of the Pyrenean sub-continental lithospheric mantle in the light of new ^{40}Ar–^{39}Ar and Sm–Nd ages on pyroxenites and peridotites (Pyrenees, France). Tectonophysics 296, 103–123.

Hirth, G., Kohlstedt, D.L., 1995. Experimental constraints on the dynamics of the partially molten upper mantle: deformation in the dislocation creep regime. J. Geophys. Res. 100, 15.441–415.449.

Holtzman, B.K., Kohlstedt, D.L., Zimmerman, M.E., Heidelbach, F., Hiraga, T., Hustoft, J., 2003. Melt segregation and strain partitioning: implications for seismic anisotropy and mantle flow. Science 301, 1227–1230.

Jung, H., Karato, S., 2001. Water-induced fabric transition in olivine. Science 293, 1460–1463.

Kelemen, P.B., Dick, H.J.B., 1995. Focused melt flow and localized deformation in the upper mantle: juxtaposition of replacive dunite and ductile shear zones in the Josephine peridotite, SW Oregon. J. Geophys. Res. 100, 423–438.

Kendall, J.-M., Pilidou, S., Keir, D., Bastow, I.D., Stuart, G.W., Ayele, A., 2006. Mantle upwellings, melt migration and the rifting of Africa: insights from seismic anisotropy. Geological Society of London, Special Publications, vol. 259, pp. 55–72.

Kisters, A.F.M., Gibson, R.L., Charlesworth, E.G., Anhaeusser, C.R., 1998. The role of strain localization in the segregation and ascent of anatectic melts, Namaqualand, South Africa. J. Struct. Geol. 20, 229–242.

Kornprobst, J., Vielzeuf, D., 1984. Transcurrent crustal thinning: a mechanism for the uplift of deep continental crust/upper mantle associations. In: Kornprobst, J. (Ed.), Kimberlites II. The mantle and Crust–Mantle Relationships. Elsevier, Amsterdam, pp. 347–359.

Lagabrielle, Y., Bodinier, J.-L., 2008. Submarine reworking of exhumed subcontinental mantle rocks: field evidence from the Lherz peridotites, French Pyrenees. Terra Nova 20, 11–21.

Le Roux, V., Bodinier, J.-L., Tommasi, A., Alard, O., Dautria, J.-M., Vauchez, A., Riches, A.J.V., 2007. The Lherz spinel lherzolite: refertilized rather than pristine mantle. Earth Planet. Sci. Lett. 259, 599–612.

Lenoir, X., Garrido, C., Bodinier, J.-L., Dautria, J.-M., Gervilla, F., 2001. The recrystallization front of the Ronda peridotite: evidence for melting and thermal erosion of subcontinental lithospheric mantle beneath the Alboran Basin. J. Petrol. 42, 141–158.

Loubet, M., Allègre, C.J., 1982. Trace elements in orogenic lherzolites reveal the complex history of the upper mantle. Nature 298, 809–814.

Mainprice, D., Tommasi, A., Couvy, A., Cordier, P., Frost, D.J., 2005. Pressure sensitivity of olivine slip systems and seismic anisotropy of the Earth's upper mantle. Nature 233, 731–733.

Monchoux, P., 1970. Les lherzolites pyrénéennes: contribution à l'étude de leur minéralogie, de leur genèse et de leurs transformations.

Monchoux, P., 1971. Comparaison et classement des massifs de lherzolite de la zone mésozoïque Nord-Pyrénéenne. Bull. Soc. Hist. Nat. Toulouse 107, 393–407.

Müntener, O., Pettke, T., Desmurs, L., Meier, M., Schaltegger, U., 2004. Refertilization of mantle peridotite in embryonic ocean basins: trace element and Nd isotopic evidence and implications for crust–mantle relationships. Earth Planet. Sci. Lett. 221, 293–308.

Pin, C., Vielzeuf, D., 1983. Granulites and related rocks in Variscan median Europe: a dualistic interpretation. Tectonophysics 93, 47–74.

Rabinowicz, M., Ceuleneer, G., 2005. The effect of sloped isotherms on melt migration in the shallow mantle: a physical and numerical model based on observations in the Oman ophiolite. Earth Planet. Sci. Lett. 229, 231–246.

Rampone, E., Piccardo, G.B., Vannucci, R., Bottazzi, P., Zanetti, A., 1994. Melt impregnation in ophiolitic peridotite: an ion microprobe study of clinopyroxene and plagioclase. Mineral. Mag. 58A, 756–757.

Rosenberg, C.L., Handy, M.R., 2000. Syntectonic melt pathways during simple shearing of a partially molten rock analogue (Norcampher–Benzamide). J. Geophys. Res. 105, 3135–3149.

Rosenberg, C.L., Handy, M.R., 2001. Mechanisms and orientation of melt segregation paths during pure shearing of a partially molten rock analog (norcamphor–benzamide). J. Struct. Geol. 23 19717-11932.

Rosenberg, C.L., Handy, M.R., 2005. Experimental deformation of partially melted granite revisited: implications for the continental crust. J. Metamorph. Geol. 23, 19–28.

Sautter, V., Fabriès, J., 1990. Cooling kinetics of garnet websterites from the Freychinède orogenic lherzolite massif, French Pyrenees. Contrib. Mineral. Petrol. 105, 533–549.

Schärer, U., Kornprobst, J., Beslier, M.O., Boillot, G., Girardeau, J., 1995. Gabbro and related rock emplacement beneath rifting continental crust: U–Pb geochronological and geochemical constraints for the Galicia passive margin (Spain). Earth Planet. Sci. Lett. 130, 187–200.
Scott, T., Kohlstedt, D.L., 2006. The effect of large melt fraction on the deformation behavior of peridotite. Earth Planet. Sci. Lett. 246, 177–187.
Spiegelman, M., 1993. Physics of melt extraction: theory, implications and applications. Philosophical Transactions: Physical Sciences and Engineering 342, 23–41.
Takei, Y., 2005. Deformation-induced grain boundary wetting and its effects on the acoustic and rheological properties of partially molten rock analogue. J. Geophys. Res. 110. doi:10.1029/2005JB003801.
Thoraval, C., Tommasi, A., Doin, M.-P., 2006. Plume–lithosphere interactions beneath a fast-moving plate. Geophys. Res. Lett. 33, L01301. doi:01310.01029/02005GL024047.
Tommasi, A., Vauchez, A., 2001. Continental rifting parallel to ancient collisional belts: an effect of the mechanical anisotropy of the lithospheric mantle. Earth Planet. Sci. Lett. 185, 199–210.
Tommasi, A., Godard, M., Coromina, G., Dautria, J.-M., Barsczus, H., 2004. Seismic anisotropy and compositionally induced velocity anomalies in the lithosphere above mantle plumes: a petrological and microstructural study of mantle xenoliths from French Polynesia. Earth Planet. Sci. Lett. 227, 539–556.
Tommasi, A., Mainprice, D., Canova, G., Chastel, Y., 2000. Viscoplastic self-consistent and equilibrium-based modeling of olivine lattice preferred orientations. Implications for upper mantle seismic anisotropy. J. Geophys. Res. 105, 7893–7908.
Tommasi, A., Tikoff, B., Vauchez, A., 1999. Upper mantle tectonics: three-dimensional deformation, olivine crystallographic fabrics and seismic properties. Earth Planet. Sci. Lett. 168, 173–186.
Tommasi, A., Vauchez, A., Fernandes, L.A.D., Porcher, C.C., 1994. Magma-assisted strain localization in an orogen-parallel transcurrent shear zone of southern Brazil. Tectonics 13, 421–437.
Tommasi, A., Vauchez, A., Ionov, D., 2008. Deformation, static recrystallization, and reactive melt transport in shallow subcontinental mantle xenoliths (Tok Cenozoic volcanic field, SE Siberia). Earth Planet. Sci. Lett. doi:10.1016/j.epsl.2008.1004.1020.
Vauchez, A., Barruol, G., 1996. Shear-wave splitting in the Appalachians and the Pyrenees: importance of the inherited tectonic fabric of the lithosphere. Phys. Earth Planet. Inter. 95, 127–138.
Vauchez, A., Garrido, C., 2001. Seismic properties of an asthenopherized lithospheric mantle: constraints from lattice preferred orientations in peridotite from the Ronda massif. Earth Planet. Sci. Lett. 192, 235–249.
Vauchez, A., Tommasi, A., 2003. Wrench faults down to the asthenosphere: Geological and geophysical evidence and thermo–mechanical effects. In: Storti, F., Holdsworth, R.E., Salvini, F. (Eds.), Intraplate strike–slip deformation belts. Geol. Soc. London Spec. Publ., London, pp. 15–24.
Vauchez, A., Dineur, F., Rudnick, R., 2005. Microstructure, texture and seismic anisotropy of the lithospheric mantle above a mantle plume: insights from the Labait volcano xenoliths (Tanzania). Earth Planet. Sci. Lett. 232, 295–314.
Vétil, J.Y., Lorand, J.P., Fabriès, J., 1988. Conditions de mise en place des felons des pyroxénites à amphibole du massif ultramafique de Lherz (Ariège, France). C. R. Acad. Sci. Paris 307, 587–593.
Vielzeuf, D., Pétrologie des écailles granulitiques de la région de Lherz (Ariège-Zone Nord Pyrénéenne). Introduction à l'étude expérimentale de l'association grenat (alm-py)-feldspath potassique. Thesis, University of Clermont-Ferrand, 1980.
Vielzeuf, D., Kornprobst, J., 1984. Crustal splitting and the emplacement of Pyrenean lherzolites and granulites. Earth Planet. Sci. Lett. 67, 87–96.
Waff, H.S., Faul, U.H., 1992. Effects of crystalline anisotropy on fluid distribution in ultramafic partial melts. J. Geophys. Res. 97, 9003–9014.
Wark, D.A., Watson, B.E., 2000. Effect of grain size on the distribution and transport of deep-seated fluids and melts. Geophys. Res. Lett. 27, 2029–2032.

Please cite this article as: Le Roux, V., et al., Feedback between melt percolation and deformation in an exhumed lithosphere–asthenosphere boundary, Earth Planet. Sci Lett. (2008), doi:10.1016/j.epsl.2008.07.053